Optical and Quantum Electronics **31:** 391–403, 1999.

Variations of relative line intensity in saturation spectroscopy due to low magnetic fields

W. K. HENSINGER, A. G. TRUSCOTT, H. RUBINSZTEIN-DUNLOP, AND N. R. HECKENBERG
Centre for Laser Science, Department of Physics, The University of Queensland, Brisbane, Queensland 4072, Australia

Received 10 December 1997; accepted 8 July 1998

Abstract. We have observed dramatic line intensity variations in the saturation spectrum of Rb^{85} and Rb^{87} due to magnetic fields of magnitude on the order of 100 nT. These variations are detected by rotation of the plane of polarisation of the pump beam and probe beam relative to the magnetic field axis. A modified rate equation model is proposed which accounts for all experimentally observed features. Our results may explain some discrepancies between theory and experiment observed by other authors. Furthermore, our study should lead to a better understanding of the processes involved in saturation spectroscopy.

Key words: atomic alignment, atomic physics, atomic spectroscopy, hyperfine structure, rubidium, saturation spectroscopy

1. Introduction

Saturation spectroscopy is a simple Doppler free method, widely used to resolve the hyperfine structure of alkali metals. There is much interest in this type of spectroscopy since it has applications in experiments involving frequency stabilisation and spectral analysis of lasers. Many studies of saturation spectroscopy have been made under various conditions. In 1980 Rinneberg *et al.* (1980) studied the crossover signal of the Na D_1 line. They found that the size of this signal was largely dependent on the atomic alignment. This alignment arose from a magnetic field (field strengths $\sim$100 μT) oriented at right angles to the electric field vector of both pump and probe beams and parallel to the beam axis. Other studies on the saturation spectroscopy of Rb have been made by Bowie *et al.* (1995) and Kim *et al.* (1997). In these studies the effect of magnetic fields (field strength $\sim$10 mT) on the relative line intensities were examined. Schmidt *et al.* (1994) carried out a thorough investigation of saturation spectroscopy in cesium. The authors found the line intensity of the cross-over $F = 2 \rightarrow F' = 2, 3$ of the D_2 line to be sensitive to magnetic fields of the order of 4 μT and reported about the role of coherent population trapping. Secondly they observed the line intensity of certain peaks to be dependent on whether the linear polarised probe and pump beams had their planes of polarisation parallel or perpendicular to each other.

Quantitative models have been proposed to calculate the relative line intensities for the different hyperfine transitions. These models generally calculate the repopulation of the degenerate Zeeman levels due to the presence of the pump beam, and then produce a spectrum via computation of the effect this repopulation has on absorption of the probe beam. Nakayama proposed one of the first models (Nakayama 1985, 1997) which used a single pumping cycle of the pump beam. Yang *et al.* (Yang and Wang 1989) extended Nakayama's ideas to include multiple pumping cycles. Both models have been experimentally tested and reasonable agreement between experiment and theory has been shown (Yang and Wang 1989; Bowie 1995). However, some discrepancies between experiment and theory have been found. In particular, Kim *et al.* (1993) observed that the influence of the geomagnetic field and laser power significantly altered the line intensities of the Rb D_2 line. Their study showed that existing models could not account for these effects and further concluded that the effects were not due to multicycling phenomena.

In this paper we investigate, for the first time to our knowledge, the effect of a very weak magnetic field (field strength $\sim 100\,\mathrm{nT}$) on the saturation spectrum of both rubidium isotopes. We show that atomic alignment resulting from the presence of the magnetic field is enough to significantly alter the line intensities of particular hyperfine transitions of the D_1 line of Rb^{85} and Rb^{87}. To model these effects a modified rate equation model is used which gives good agreement with our experiment.

2. Theory

In a simple two level atom, optical coherences between the ground and excited state are an inherent feature of saturation spectroscopy, caused by the high power density necessary to achieve at least partial saturation. However, alkali atoms such as rubidium have two hyperfine ground states and thus optical pumping between ground states is possible. This mechanism therefore plays an integral role and ensures a large probing signal even for exceedingly low pump intensities. In this regime, rate equations rather than Bloch equations are used to calculate the relative line strengths.

In Nakayama's rate equation model the relative intensities I after one pumping cycle are calculated using

$$I_{ij} = |\mu_{\mathrm{pr}}|^2 \left(-|\mu_{\mathrm{pu}}|^2 \delta_{\mathrm{pu,sp}} + \frac{|\mu_{\mathrm{pu}}|^2 |\mu_{\mathrm{sp}}|^2}{\Gamma} \right) \tag{1}$$

where $|\mu_{\mathrm{pu}}|^2, |\mu_{\mathrm{pr}}|^2, |\mu_{\mathrm{sp}}|^2$ are the transition probabilities calculated with the Wigner–Eckart theorem, for the pump, the probe and the spontaneous emission from the excited state to the ground state, respectively. Γ is the total

transition probability of each Zeeman sublevel, thus $|\mu_{sp}|^2/\Gamma$ indicates the branching ratio of the spontaneous emission from the upper state. By summing over all possible transitions i, j between degenerate Zeeman sublevels one can calculate the line intensity I of a certain hyperfine transition.

The number of pumping cycles that an atom undergoes due to the pump beam is obtained by calculating the number of absorptions per unit time and multiplying this with the time an atom spends in the beam. Furthermore, pumping with the probe beam is possible, if the intensity of the probe beam is large enough. For the experiments presented here, the lowest number of expected pumping cycles of the pump beam is four. Therefore the multipumping cycle model proposed by Yang and Wang forms the basis of our model.

Our theory pertains to the experimental arrangement shown in Fig. 1. A small magnetic field is oriented at 90° to the propagation of both the probe and pump beams. The probe and pump beams are linearly polarised and their plane of polarisation can be rotated via rotation of independent half wave plates. The percentage of π polarised light depends on the component of the electric field vector parallel to the direction of the magnetic field and similarly the percentage of $(\sigma^+ + \sigma^-)/2$ polarised light depends on the component of the electric field vector perpendicular to the magnetic field (see Fig. 1). It follows

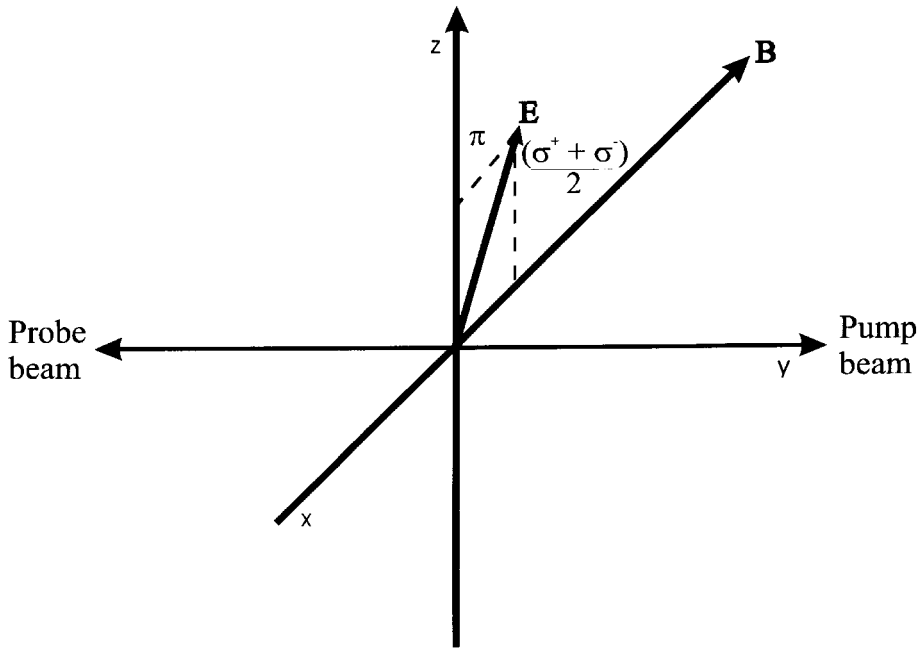

Fig. 1. Component of electric field vector parallel to the magnetic field direction induces π transitions. Component of electric field vector perpendicular to the magnetic field direction induces $(\sigma^+ + \sigma^-)/2$ transitions. If the direction of B-Field lies in a plane, perpendicular to the direction of beam propagation, the percentage of π polarised light can be varied from 0 – 100 by rotating the plane of polarisation.

then that by changing the plane of polarisation or by changing the direction of the applied magnetic field the percentage of π and $(\sigma^+ + \sigma)^-/2$ polarised light in both the pump and probe beams can be varied. Following Yang and Wang (1989), but incorporating a varying amount of π light in pump and probe beams, as well as allowing pumping by the probe beam, the signal intensity $S_{FF'}$ for a transition between hyperfine levels F and F' after m pumping cycles of the pump and n pumping cycles of the probe can be written as

$$S_{FF'}(\omega, m, n, y, z) = \left[1 - \frac{\sum_{ij} P_i(m,n,y,z)|\mu_{ij}|^2 \delta_{i,j} z}{s_{FF'}} + \frac{\sum_{ij} P_i(m,n,y,z)|\mu_{ij}|^2 (\delta_{i,j+1} + \delta_{i,j-1})(1-z)/2}{s_{FF'}}\right] \times \frac{(\gamma/2)^2}{(\omega_{FF'} - \omega)^2 + (\gamma/2)^2} \times I_{FF'} \tag{2}$$

where

$$s_{FF'} = \sum_{ij} P_i(0,0,y,z)|\mu_{ij}|^2 \delta_{i,j} z + P_i(0,0,y,z)|\mu_{ij}|^2 (\delta_{i,j+1} + \delta_{i,j-1}) \frac{(1-z)}{2} \tag{3}$$

In this equation $P_i(m,n,y,z)$ represents the population of the Zeeman sublevel i after m pumping cycles of the pump beam and n pumping cycles of the probe beam, $|\mu_{ij}|^2$ are the transition probabilities from a state i to state j, z is the fraction of π polarised light of the probe beam due to the orientation of its electric field vector with respect to the magnetic field axis, $I_{FF'}$ is a coefficient which represents the total transition strength between the two hyperfine levels F and F$'$ and $s_{FF'}$ gives the absorptions signal in case of no pumping of the pump and probe beam and γ is the natural linewidth for the transition.

To calculate the level population we modify the Yang and Wang model (Yang and Wang 1989) to incorporate pumping by the probe and pump beam, as well as to allow different percentages of π light for both pump and probe beam. Thus the level populations are given by

$$\begin{aligned} P_i(m+1,n,y,z) = \sum_{kj} \Big[& P_k(m,n,y,z)|\mu_{kj}|^2 \delta_{kj} |\mu_{ji}|^2 y \\ & + P_k(m,n,y,z)|\mu_{kj}|^2 (\delta_{k,j+1} + \delta_{k,j-1})|\mu_{ji}|^2 \frac{(1-y)}{2}\Big] \\ & + P_i(m,n,y,z) - \sum_j \Big[P_i(m,n,y,z)|\mu_{ij}|^2 \delta_{i,j} y \\ & + P_i(m,n,y,z)|\mu_{ij}|^2 (\delta_{i,j+1} + \delta_{i,j-1}) \frac{(1-y)}{2}\Big] \end{aligned} \tag{4}$$

$$P_i(m,n+1,y,z) = \sum_{kj} \Big[P_k(m,n,y,z)|\mu_{kj}|^2 \delta_{kj} |\mu_{ji}|^2 z + P_k(m,n,y,z)|\mu_{kj}|^2 (\delta_{k,j+1} + \delta_{k,j-1})|\mu_{ji}|^2 \frac{(1-z)}{2} \Big] + P_i(m,n,y,z) - \sum_{j} \Big[P_i(m,n,y,z)|\mu_{ij}|^2 \delta_{i,j}\, z + P_i(m,n,y,z)|\mu_{ij}|^2 (\delta_{i,j+1} + \delta_{i,j-1}) \frac{(1-z)}{2} \Big] \quad (5)$$

The probability for spontaneous emission is normalized to the sum of all probabilities to fall into any other Zeeman state of either lower hyperfine level. This is done to introduce a leak factor caused by optical pumping from one ground state to the other. y is the fraction of π light present in the probe beam due to the orientation of its electric field vector with respect to the magnetic field direction. To implement pumping by the probe beam we calculate the ratio α of the pump to probe scattering rate and then include one pump cycle of the probe after every α pump cycles of the pump beam. For example, if the pump beam is 10 times more likely to scatter photons than the probe beam we include one pumping cycle of the probe for every 10 pumping cycles of the pump.

To illustrate the theory, we analyze theoretically the $F = 2 \rightarrow F' = 1$ transition of Rb^{87}. Fig. 2 shows the Zeeman level populations of the $F = 2$ ground state after two pumping cycles of the pump beam. In these calculations we assume that all Zeeman levels have an equal initial population, the

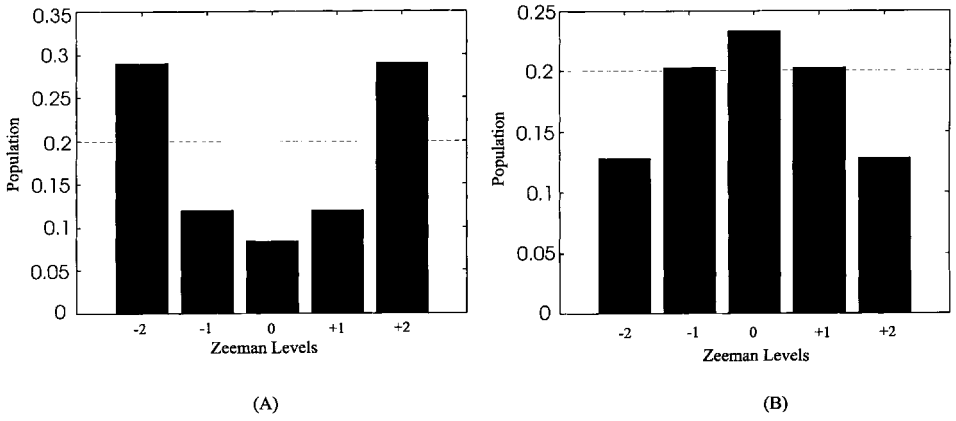

Fig. 2. Zeeman level populations of a $F = 2 \rightarrow F' = 1$ transition after two pumping cycles for (A) π pumping and for (B) $(\sigma^+ + \sigma^-)/2$ pumping.

initial populations are represented in Fig. 2 by a dashed line. In part (A) of Fig. 2 the pump beam excites just π transitions, while in part (B) it excites only $(\sigma^+ + \sigma^-)/2$ transitions. The results show that pumping with π light leads to an accumulation of atoms in the outer most Zeeman levels, while $(\sigma^+ + \sigma^-)/2$ pumping preferentially populates the $m_F = 0$ Zeeman sublevel. These trends continue for larger numbers of pumping cycles causing total accumulation of atoms in the outer most Zeeman levels for condition (A), and accumulation of atoms in the $m_F = 0$ Zeeman sublevel for condition (B). It is this accumulation in particular Zeeman sublevels that gives rise to dramatic differences in the saturation spectrum for a particular probe polarisation, since absorption by particular Zeeman population distributions is more probable for certain probe polarisations. To illustrate this point we calculate the relative line strengths of D_1 line for both Rb^{85} and Rb^{87} using two pumping cycles of the pump beam and no pumping of the probe beam. These results are shown in parts (A) and (B) of Fig. 3. Fig. 3 (A) shows the results for a pump beam that excites only π transitions while (B) shows the results for a pump beam that excites only $(\sigma^+ + \sigma^-)/2$ transitions. Both (A) and (B) spectra are produced using a $(\sigma^+ + \sigma^-)/2$ polarised probe beam. The differences in the two calculated spectra are dramatic. In particular there are significant differences in the effects on the line intensity of peak 1 ($F = 2 \rightarrow F' = 1$, Rb^{87}), peak 3 ($F = 2 \rightarrow F' = 2$, Rb^{87}), peak 4 ($F = 3 \rightarrow F' = 2$, Rb^{85}), peak 6 ($F = 3 \rightarrow F' = 3$, Rb^{85}) and on the cross-over peaks 2 ($F = 2 \rightarrow F' = 1, 2$, Rb^{87}) and 5 ($F = 3 \rightarrow F' = 2, 3$, Rb^{85}). The variations in the line intensities can be qualitatively explained as follows. For $F \rightarrow F' = F - 1$ transitions, pumping with π polarised light leads to a large population in the outer most Zeeman sublevels. This population can only be detected using a probe beam that excites $(\sigma^+ + \sigma^-)/2$ transitions. Furthermore, the probability for an atom in the outer most positive m_F

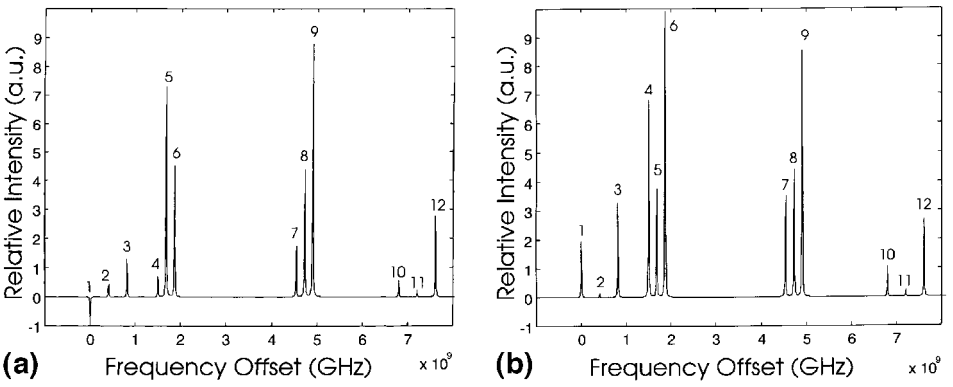

Fig. 3. Calculated D_1 line of Rb after two pumping cycles of the pump beam and no pumping of the probe beam. Pump beam excites either (A) π or (B) $(\sigma^+ + \sigma^-)/2$ while the probe beam excites only $(\sigma^+ + \sigma^-)/2$ transitions.

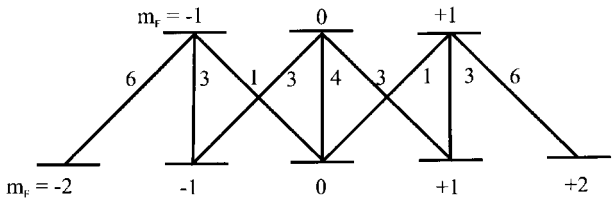

Fig. 4. Zeeman transition probabilities for a $F = 2 \rightarrow F' = 1$ transition.

Zeeman level to absorb a σ^- photon is large (see Fig. 4). Similarly the probability for an atom in the outer most negative m_F Zeeman level to absorb a σ^+ photon is large. Thus one should expect a large amount of probe absorption to take place for peaks 1 and 4 in Fig. 3 (A).

For the same transitions, except now considering a $(\sigma^+ + \sigma^-)/2$ polarised pump beam the population accumulates in the inner Zeeman levels, while the outer Zeeman level populations are reduced. In this situation we except that the probe beam will undergo much less absorption that in (A), and thus peaks 1 and 4 are considerably larger in the calculated spectrum shown in (B). In (A) it can be seen that peak 1 is inverted. The repopulation due to the pump beam increases the absorption of the probe beam, compared with the absorption of the probe beam without pumping. A similar argument can be used to explain the difference in peak heights for $F \rightarrow F' = F$ transitions. To illustrate our model more clearly we show the line intensity of peak 1 as a function of angle of the pump and probe half wave plate in Fig. 5.

3. Experimental set-up

The experimental set-up is shown in Fig. 6. We use a 30 mW Sharp laser diode (LTO-24MD). The laser is stabilized using optical feedback from a holographic diffraction grating [8] and has a free running linewidth of around 1.4 MHz. The temperature of the laser diode is controlled using a PID servo loop which regulates the diode temperature to ± 40 μK. A low noise current controller provides the junction current needed to drive the laser diode [9]. Tuning of the laser frequency over a 9 GHz range is possible by ramping the voltage applied to a piezo electric transducer (PZT) located behind the diffraction grating.

Our experiments take place inside a 10 cm Rb vapour cell. The cell is located inside a magnetic shield and orientated so as to be at right angles to the Earths magnetic field. Both the pump and probe beams are linearly polarised and their plane of polarisation (direction of electric field) vector can be varied relative to the magnetic field direction via rotation of independent half wave plates. These two counterpropagating beams are overlapped inside the cell. The probe beam is detected using a photodiode PD_2. A third beam

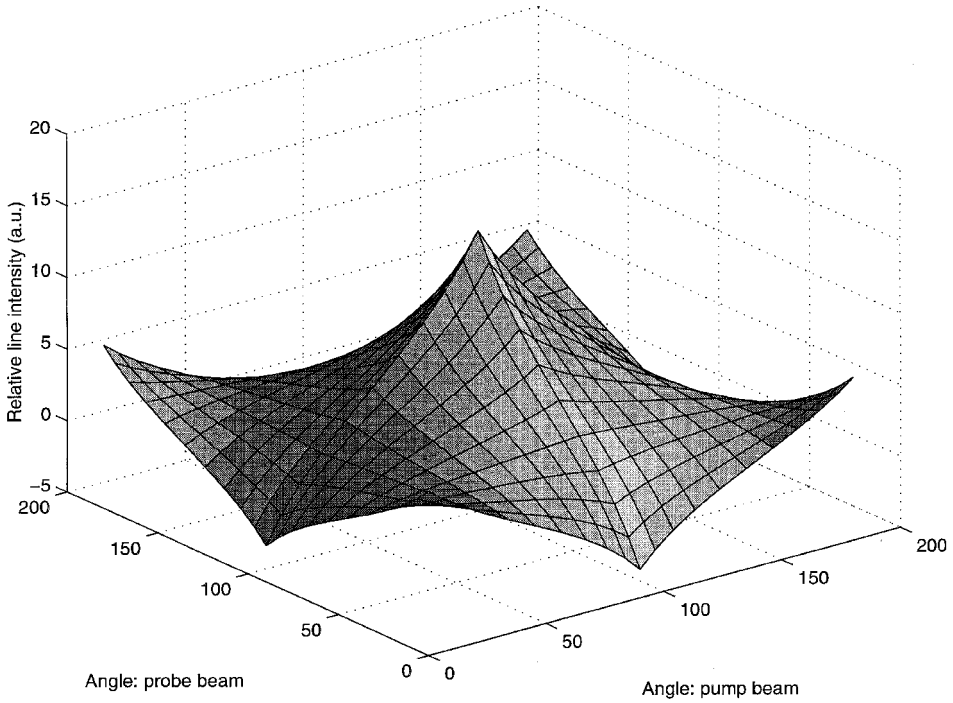

Fig. 5. Relative line intensity of peak 1 (Rb^{87} $F = 2 \rightarrow F' = 1$) as a function of angle between E-vector and B-vector in both pump and probe beam. An offset of 90 degrees was added to each angle.

nearly equal in intensity to the probe beam is passed through the cell and facilitates subtraction of the Doppler background and noise from the probe signal. This beam is detected with photodiode PD_1.

The total power used in the experiment can be varied by rotation of a polariser relative to the polarisation axis of the laser diode output beam. Also, the ratio of pump power is controlled using half wave plate in conjunction with a polarising beamsplitting cube (PBSC).

To shied the Earth's magnetic field we use a μ-metal cage. This cage consists of 5 sheets of AD-MU-80 each of thickness 0.25 mm concentrically rolled. Each μ-metal sheet is separated from its neighbour by a mylar layer of thickness 0.8 mm. The resulting cylinder has a radius of 3.5 cm and a length of 31.5 cm. According to the manufacturer's (AD-Vance magnetics) specifications, such a shield should provide 40 dB attenuation of any magnetic field oriented at right angles to the axis of the cylinder. The magnitude of the geomagnetic field in our laboratory is approximately 50 μT, thus we expect that inside the shield there is a 5 nT magnetic field present. However, magnetic field measurements using a flux gate magnetometer indicate that a field of about 100 nT remains. To shield magnetic fields aligned along the axis of our cylindrical cage we use μ-metal end caps that have small holes to allow laser access.

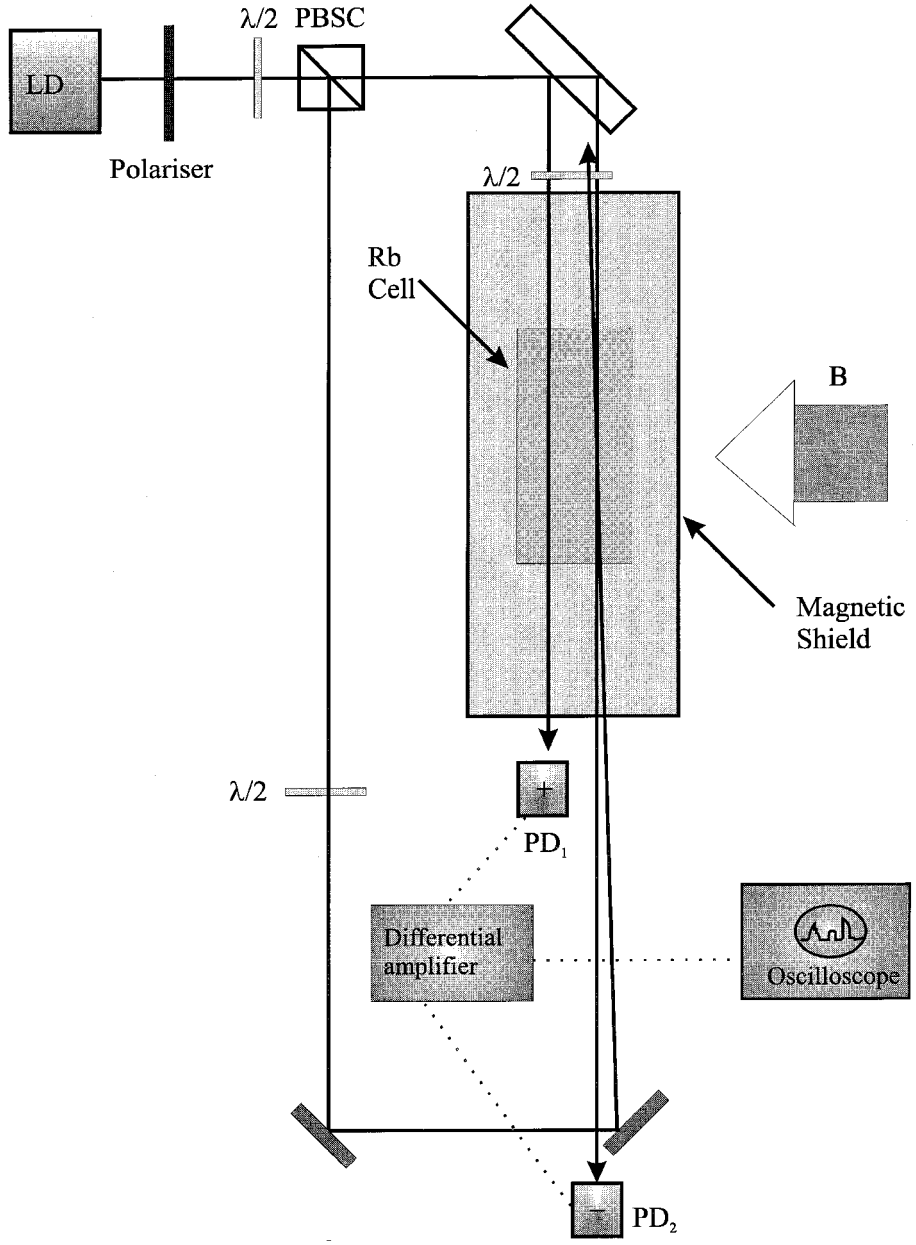

Fig. 6. Schematic of experimental setup showing orientation of the geomagnetic field in relation to the beam axis.

4. Experimental results

In our investigations we have used a wide range of pump and probe intensities and have found good agreement between theory and experiment over

this range of intensities. Here we present the results of two representative experiments to compare our theoretical model with experimentally observed line intensity variations. In the first experiment we monitored the amplitude of two peaks, peak 1 ($F = 2 \rightarrow F' = 1$, Rb^{87}) and peak 4 ($F = 3 \rightarrow F' = 2$, Rb^{85}) for two different probe polarisations. The probe and pump beam intensities for this experiment are 3 $\mu W/mm^2$ and 12 $\mu W/mm^2$ respectively, thus we refer to this experiment as a low intensity experiment. The second experiment is similar to the first, with some exceptions. We monitor the amplitude of only peak 1 and use a probe intensity of 66 $\mu W/mm^2$ and a pump intensity of 114 $\mu W/mm^2$ (which we refer to as a high intensity experiment). The experimental procedure is as follows: the probe and pump beam polarisation are aligned so that the peak under consideration is minimised. In this configuration the pump beam polarisation is assumed to be perpendicular to the magnetic field and thus excites only $(\sigma^+ + \sigma^-)/2$ transitions while the probe beam polarisation is parallel to the magnetic field and excites only π transitions. The plane of polarisation of the pump beam is now rotated and the variation of the peak height recorded as a function of pump polarisation. An equivalent experiment is carried out for a $(\sigma^+ + \sigma^-)/2$ polarised probe beam.

The results for the low intensity experiment are shown in Fig. 7. In this figure (A) and (B) are the line intensities of peak 1 as a function of pump polarisation, and (C) and (D) are the line intensities of peak 4 as a function of pump polarisation. (B) and (D) are for a $(\sigma^+ + \sigma^-)/2$ polarised probe beam and (A) and (C) are for a π polarised probe beam. The solid line on each graph is the prediction our theoretical model using four pump cycles of the pump beam and zero pump cycles of the probe beam ($m = 4$, $n = 0$).

Fig. 8 shows the results for the high intensity experiment. Fig. 8 (A) shows the variation of the amplitude of peak 1 as a function of pump polarisation, for a π polarised probe beam while part (B) is for $(\sigma^+ + \sigma^-)/2$ polarised probe beam. The model parameters used to produce the solid lines are $m = 8$, $n = 2$ pumping cycles.

Our results show good agreement between theory and experiment in both low and high intensity regimes. The data obtained with a $(\sigma^+ + \sigma^-)/2$ polarised probe beam does however show some variation from the theoretical predictions. This can be observed in the low intensity data for the regions of higher $(\sigma^+ + \sigma^-)/2$ pump beam polarisation. This trend is most probably due to a systematic error in the data. Possible systematic errors include: imperfect overlapping of pump and probe beams and the presence of magnetic fields aligned along the beam axis which cause $(\sigma^+ + \sigma^-)/2$ transitions to be excited. Another systematic error occurs in our calculations. Atoms might pass multiple times through the pump and probe beams and thus may lead to unequal initial Zeeman populations.

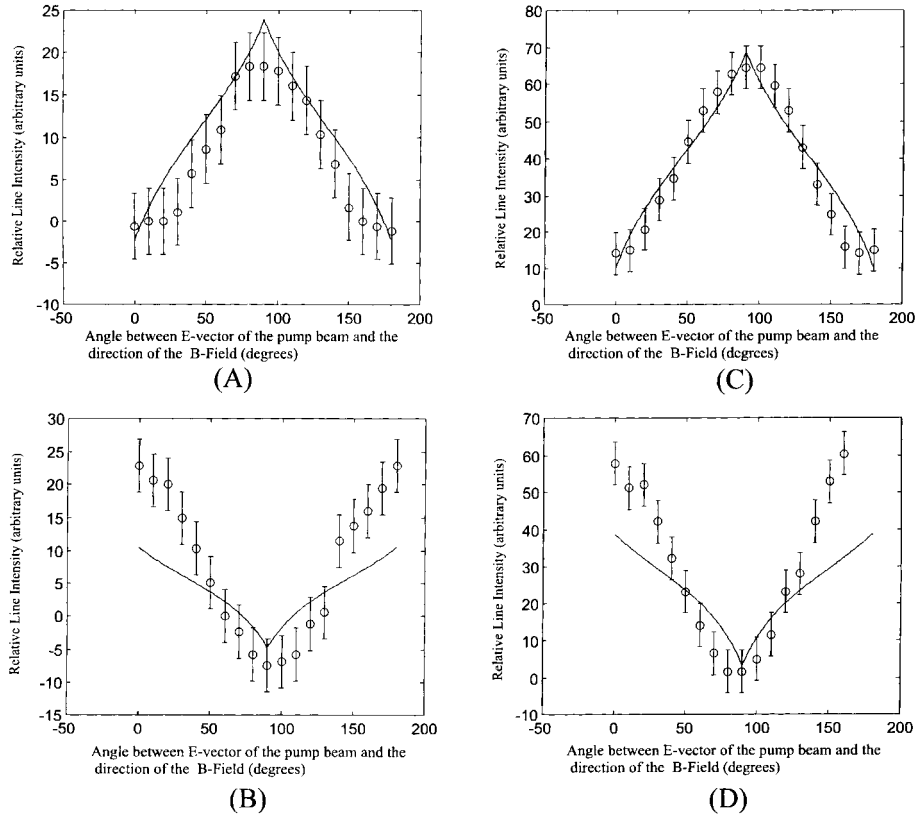

Fig. 7. Comparison between low intensity experimental data and theoretical predictions. An angle of 90° corresponds to a π polarised pump beam. (An offset of 90° was added to this angle) (A) and (B) are for peak 1 ($F = 2 \rightarrow F' = 1$), (C) and (D) are for peak 2 ($F = 3 \rightarrow F' = 2$), (A) and (C) are with a π probe beam, (B) and (D) are with a $(\sigma^+ + \sigma^-)/2$ probe beam.

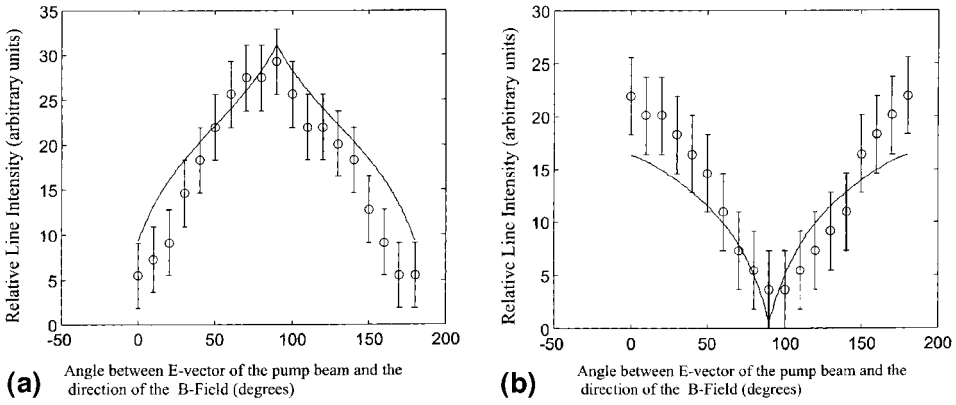

Fig. 8. Comparison between high intensity experimental data and theoretical predictions. An angle of 90° corresponds to a π polarised pump beam. (An offset of 90° was added to this angle) (A) and (B) are for peak 1 ($F = 2 \rightarrow F' = 1$), (A) is with a π probe beam, (B) is with a $(\sigma^+ + \sigma^-)/2$ probe beam.

In addition to the features of the experiment already discussed; we observe that peaks 1 and 4 have their minimum or a maximum line intensity at a common angle of probe and pump half wave plate. This behavior is predicted by the theory for peaks 1 and 4. Furthermore, our model predicts that the crossover peaks 2 and 5 will also have maxima and minima at common angles, different to the common angle for peak 1 and 4. This is also observed in the experiment.

We also experimentally observe the pumping effect of a high intensity probe beam. By aligning pump and probe half wave plates to an angle at which peak 1 was inverted we were able to investigate the effect of attenuation of the probe beam on the inversion. When the probe beam is attenuated by approximately 90% of its original value the line intensity of peak 1 becomes positive. This measurement is done at intensities still far below saturation intensity I_{sat} which equals approximately 1.5 mW/cm^2 for the D_1 line of Rb using $I_{\text{sat}} = hc/\tau\lambda^3$ [10], where h is the Planck constant, c is the speed of light, τ the spontaneous lifetime and λ the wavelength of the transition. This result indicates that a significant amount of the repopulation is done by the probe beam, which leads to the inversion of the peak. Therefore even at probe intensities below saturation, pumping effects of the probe beam should be included in the model.

5. Conclusion

Our investigation leads to a better understanding of line intensities in saturation spectroscopy of Rb which can be also used for the analysis of other alkali metals. It shows that the orientation of the plane of polarisation (direction of the electric field vector) of probe and pump beam relative to the direction of even weak magnetic fields affects the relative line intensities in saturation spectroscopy. Furthermore, the intensity of both the probe and pump beams must be carefully controlled to enable satisfactory theoretical predictions about line intensities. The sensitive behaviour of line intensities may have some interesting applications, for example detection of very weak magnetic fields. Further investigation into these applications in progress.

Acknowledgements

The corresponding author (W.K.H.) would like to express his gratitude to the Friedrich–Ebert–Stiftung for their financial support. We would also like to acknowledge the expert technical assistance of the Physics Department workshops.

References

Rinneberg, H., T. Huhle, E. Matthias and A. Timmermann, *Atoms and Nuclei*. **295** 17, 1980.
Jason Bowie, Jack Boyce and Raymond Chiao, *J. Opt. Soc. Am.* **12**(10) 1839, 1995.
Kim J.B., H.A. Kim, H.S. Moon and H.S. Lee, *J. Opt. Soc. Am.* **14**(11) 2946, 1997.
Shigeru Nakayama, *Jn. J. Appl. phys.* **24**(1) 1, 1985.
Shigeru Nakayama, *Physica Scripta.* **T70** 64, 1997.
Dong-Hai Yang and Yi-Qiu Wang, *Opt Commun.* **74**(1,2) 54, 1989.
Seung-Sub Kim, Sang-Eon Park, Ho-Seong Lee, Cha-Hwan Oh, Jong-Dae Park and Hyuck Cho, *Jn. J. Appl. Phys.* **32**(7) 3291, 1993.
Macadam, K.B., A. Steinbach and C. Wieman, *Am. J. Phys.* **60**(12) 1098, 1992.
Libbrecht, K.G. and J.I. Hall, *Review of Scientific Instruments*, **64**(8) 2133, 1993.
Adams, C.S., M. Sigel and J. Mlynek, *Physics Reports.* **240** 143, 1994.
Schmidt, O., K.-M. Knaak, R. Wynands and D. Meschede, *Appl. Phys. B*, **59** 167, 1994.